Journal of Membrane Science 475 (2015) 1–8

Contents lists available at ScienceDirect

Journal of Membrane Science

journal homepage: www.elsevier.com/locate/memsci

Preparation, characterization and performance enhancement of polysulfone ultrafiltration membrane using PBI as hydrophilic modifier

Erdal Eren*, Adem Sarihan, Bilge Eren, Huseyin Gumus, Fadime Ozdemir Kocak

Bilecik Seyh Edebali University, Faculty of Science and Arts, Department of Chemistry, 11210 Bilecik, Turkey

ARTICLE INFO

Article history:
Received 27 August 2014
Received in revised form
1 October 2014
Accepted 5 October 2014
Available online 14 October 2014

Keywords:
Polybenzimidazole
Blend membrane
Polysulfone
Hydrophilic modification
Ultrafiltration

ABSTRACT

In this study, new type of polysulfone (PSf) composite ultrafiltration membranes were prepared by blending PSf with poly[2,2′-(m-phenylene)-5,5′-dibenzimidazole] (PBI). The prepared membranes were characterized by water contact angle, SEM, FTIR, DSC, TG/DTG and cross-flow filtration techniques. We demonstrated that membrane characteristics such as porosity, hydrophilicity and thermal stability of PSf can be significantly enhanced with the incorporation of PBI. The composite membranes exhibited comparable bovine serum albumin (BSA) retention (69% vs. 36%) and water fluxes (355 vs. 228 L/m^2 h) against pristine PSf membranes.

1. Introduction

Ultrafiltration (UF) membrane technology has vast applications in various industrial processes such as in food, pharmaceutical, biotechnological, pure water production and seawater desalination [1–4]. The hydrophilicity, porosity and surface roughness as well as mechanical strength of UF membrane plays an important role in membrane separation process [5]. Polysulfone (PSf) is widely used as a material for the UF membrane because of its excellent balance among the chemical and mechanical properties [6,7]. But, the use of PSf membranes is restricted due to its hydrophobicity. Hydrophobic properties of PSf membranes result in low water flux and serious membrane fouling caused by interactions with hydrophobic solutes. Therefore, different methods have been developed to obtain hydrophilic PSf membranes, such as blending with hydrophilic polymers [8–10], grafting with other polymers [11,12]. Due to its simplicity, polymer blending is an attractive technique for the design of new PSf membranes [8–10]. But, most of polymers form immiscible blends due to the effects of intermolecular interactions between unlike polymer pairs.

Poly[2,2′-(m-phenylene)-5,5′-dibenzimidazole] (PBI) has both proton donor (–NH–) and proton acceptor (–N=) hydrogen bonding sites. Due to the donor and acceptor hydrogen-bonding sites, PBI forms miscible blends with different polymers [13,14]. PBI is also known to absorb 15 mass% water at equilibrium and the water in PBI is mobile [15]. These properties of PBI make it a promising membrane blending material for the UF applications. By using PBI additive in PSf, the various properties of PSf membrane such as hydrophilic–hydrophobic balance and morphology can be easily altered. These blend membranes can exhibit a better solute selectivity and water permeability in comparison to hydrophobic polysulfone due to the improvement in hydrophilicity.

Although a lot of studies have been performed to modify the PSf membranes by addition of different additives, to our best knowledge there is no report about investigation of PBI addition effect on morphology and properties of PSf membranes. Therefore, the aim of this study is to examine the effect of PBI addition, a polybenzimidazole, into the casting solution for improving the performance of PSf membrane. In order to characterize the prepared membranes, water contact angle, scanning electron microscopy (SEM), Fourier transform infrared spectroscopy (FTIR), differential scanning calorimetry (DSC), thermogravimetry (TG), derivative thermogravimetry (DTG) and

Table 1
Preparation conditions for polysulfone membranes.

Membrane	Casting solution (wt%)			
	PSf	NMP	PEG 400	PBI
M0	17	73.00	10	0
M1	17	72.75	10	0.25
M2	17	72.50	10	0.50
M3	17	72.00	10	1.0

* Corresponding author. Tel.: +90 228 214 1480; fax: +90 228 214 1162.
E-mail address: erdal.eren@bilecik.edu.tr (E. Eren).

http://dx.doi.org/10.1016/j.memsci.2014.10.010
0376-7388/

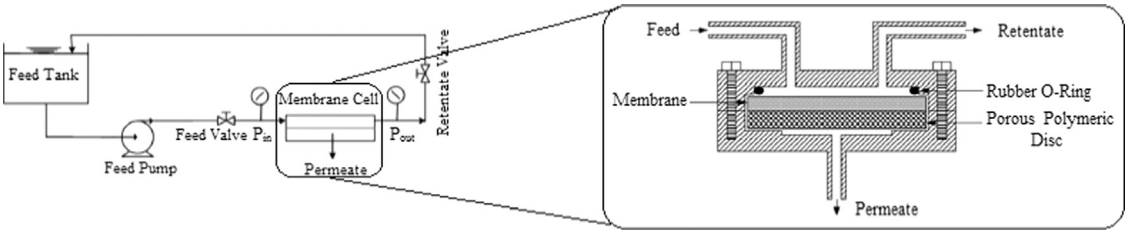

Scheme 1. Schematic diagram of the cross-flow filtration cell module.

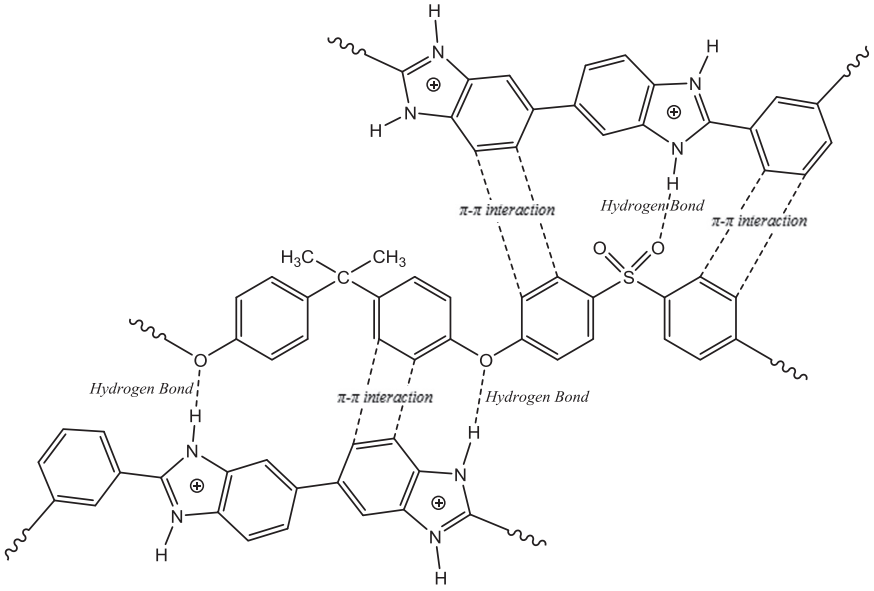

Scheme 2. Possible H-bonding and π–π interactions between the functional groups of the PSf and PBI.

cross-flow filtration measurements were employed. The rejection performances of prepared PSf/PBI blend membranes were also determined using bovine serum albümin (BSA) as a model protein.

2. Experimental

2.1. Materials and instrumentation

PSf (M_w=22.000 g/mol), *N*-methyl-2-pyrrolidone (NMP) and polyethylene glycol 400 (PEG-400) from Sigma-Aldrich Co. (USA) were used in the casting solution as the base polymer, the solvent and pore former, respectively. 3,3′-diaminobenzidine tetrahydrochloride (DAB · 4HCl · $2H_2O$), polyphosphoric acid (PPA, 85% P_2O_5), isophthalic acid (IPA), and bicarbonate was purchased from Sigma-Aldrich Co. (USA). Bovine serum albümin (BSA, M_w ~66 KDa) was obtained from Bioshop, Canada.

The water contact angles for prepared membranes were determined at room temperature using sessile droplet method by a KSV Attension contact angle analyzer. At least five angles were measured for each sample and then the average value was calculated and reported. Exstar DSC 7020 differential scanning calorimeter was used to investigate the miscibility of polymers. A typical sample weight was about 5 mg and the scan speed was 20 °C/min under nitrogen atmosphere. FTIR spectra of the polymer were recorded in the region 3800 to 1000 cm^{-1} on a Spectrum-100 FTIR spectrometer. The TG and DTG curves were obtained using a Seiko Exstar 7200 thermal analyser under air atmosphere. The morphologies of membranes were examined by SEM (Carl Zeiss ULTRA Plus). The concentration of BSA was estimated with UV–vis. spectrometer (PG instruments, T80) at λ_{max}=280 nm wavelength.

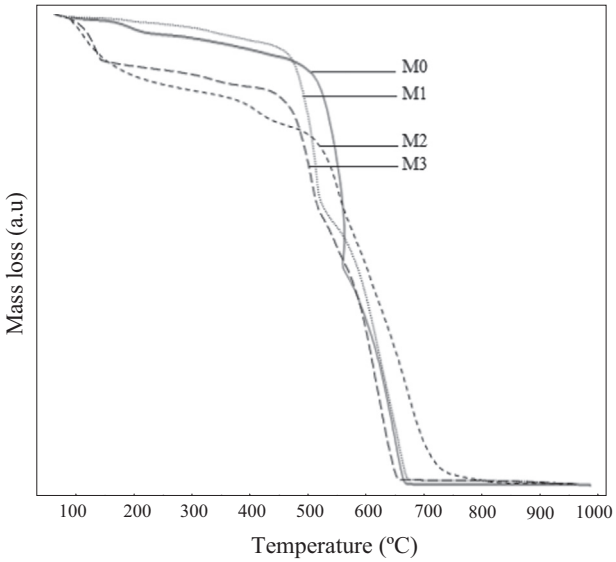

Fig. 1. TG curves of PSf and PSf/PBI blend membranes obtained at a heating rate of 10 °C min^{-1} in static air atmosphere.

2.2. Methods

2.2.1. Preparation of PBI

In a 500 mL round bottom flask equipped with a screw cap and a mechanical stirrer, DAB · 4HCl · $2H_2O$ was gradually added to dissolve in PPA under nitrogen atmosphere at about 140 °C. After eliminating the hydrochloride, IPA was added into the solution and

Table 2
TG/DTA and T_g characteristics of PSf and PSf/PBI blend membranes.

Heating rate (°C/min)	M0			M1			M2			M3		
	5	10	15	5	10	15	5	10	15	5	10	15
T_{onset} (°C)	448	431	439	390	410	415	394	422	424	338	399	404
T_{max1} (°C)	520	542	556	483	511	526	480	522	535	471	502	520
T_{max2} (°C)	605	634	653	596	623	628	605	627	678	591	617	638
$(d\alpha/dt)_{max1}$(%/min)	8.12	21.0	33.0	3.60	9.1	15.0	3.78	12.0	20.2	3.18	6.88	3.00
$(d\alpha/dt)_{max2}$(%/min)	4.82	5.94	7.20	3.70	5.20	6.20	4.99	5.79	6.66	4.42	6.80	8.23
T_g (°C)	147			150			151			157		

T_{onset} represents the onset temperature and T_{max} represents the temperature at the maximum mass-loss rate $(d\alpha/dt)_{max}$. The subscripts 1 and 2 represent the first and second stages of degradation, respectively. T_g glass symbolizes transition temperatures of PSf/PBI blend membranes.

the temperature was increased to 170 °C thoroughly. The reaction system was fixed at 170 °C for about 20 min first; it was afterwards heated at 200 °C to perform the polycondensation. The obtained polymer was then isolated immediately by pouring into distilled water. A saturated solution of sodium bicarbonate was then added to neutralize the remained acid. It was afterwards filtered and washed with water till the pH value of the washing water was about 7. The polymer was finally obtained by drying at 120 °C for at least 24 h.

2.2.2. Preparation of membrane

Pristine PSf membrane casting solution was prepared as follows: PSf (1.7 g) was completely dissolved in NMP solvent (7.30 g) at 60 °C, (ii) PEG as pore former (1.0 g) were added into the PSf solution and stirred for 24 h 60 °C. PSf/PBI blend membranes were prepared as follows: PSf (1.7 g) was completely dissolved in NMP solvent (4.0 g) at 60 °C, PEG as pore former (1.0 g) were added to the PSf solution and stirred for 24 h 60 °C, (ii) then, PBI (0.25, 0.50 and 1.00 g) were dissolved in NMP (3.05, 2.80, 2.30 g) at 100 °C for 12 h respectively. Then PBI solutions were added PSf solutions and the final solutions were stirred at 60 °C for 12 h in order to obtain different PBI content membrane casting solutions.

The membranes were prepared by casting the polymer solutions uniformly on glass plate (15 cm × 15 cm) using a home-made casting knife with a knife gap set at 200 μm. Casting was done at 25 °C. After casting, membranes were kept in open air for 10 s to evaporate the solvent and then the casted film along with glass plate was gently immersed into the bath including ultra pure water. The prepared membranes were kept in pure water for more than 12 h to remove residual solvent before test. For all the casting solutions, the mass content of PSf and PEG to total casting solution was 17 and 10 mass%, respectively, and the mass content of PBI to total casting solution was varied from 0 to 1.0 mass%. The prepared membranes with 0 and 1.0 mass% PBI contents in the casting solutions were designated as M0, M1, M2 and M3 (Table 1).

2.3. Characterization of membranes

All the permeation and rejection experiments were carried out in home-made cross flow ultrafiltration cell (Scheme 1) with a membrane diameter of 47 mm.

2.3.1. Water uptake and porosity

Water uptake properties of the membranes were measured as follows. The membranes were soaked in water for 24 h and weighed after mopping with blotting paper. These wet membranes were dried in a vacuum oven, at 40 °C for 24 h and the dry weights of the membranes were determined. From the dry and wet weights of the samples, the percent of water uptakes were

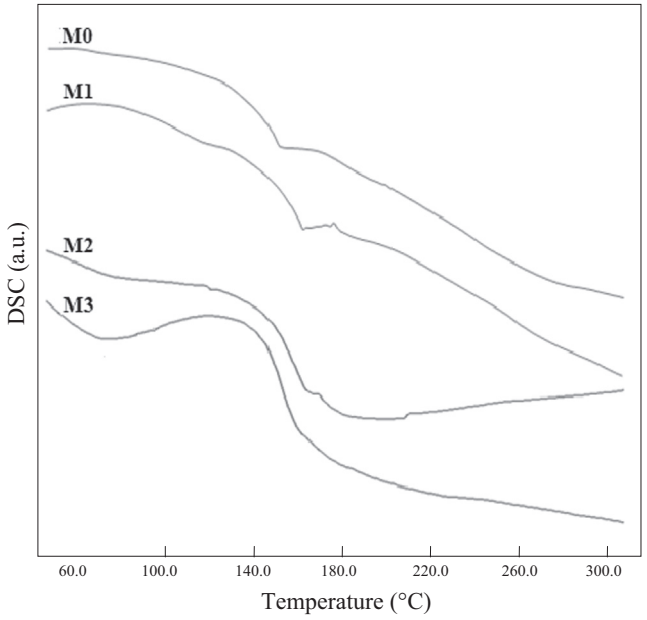

Fig. 2. DSC thermograms of PSf and PSf/PBI blend membranes.

calculated using the following equation:

$$\%\ \text{Water uptake} = \frac{W_w - W_d}{W_d} \times 100 \quad (1)$$

where W_w is the wet membrane's weight, W_d is the dry membrane's weight.

Porosity was measured from the dry and wet weights of the samples by using the following equation:

$$\%\ \text{Porosity} = \frac{W_w - W_d}{dA\delta} \times 100 \quad (2)$$

where W_w is the wet membrane's weight, W_d is the dry membrane's weight, d is the density of water in wet membrane at 25 °C (the measured temperature) and A is the area of membrane in wet state (cm^2) and δ is the thickness of membrane in wet state (cm).

2.3.2. Pure water flux and membrane hydraulic resistance

The pure water flux (PWF) was measured by direct measurement of the permeate flow (L/m^2 h). The PWF was measured at different transmembrane pressures such as 80, 150, 200, 250 and 300 kPa after the compaction time of 12 h.

$$J_w = \frac{Q}{A\Delta t} \quad (3)$$

where J_w is the flux (L/m^2 h), Q ist the quantity of permeate collected (L), A is the effective membrane surface area (m^2) and Δt is the sampling time (h).

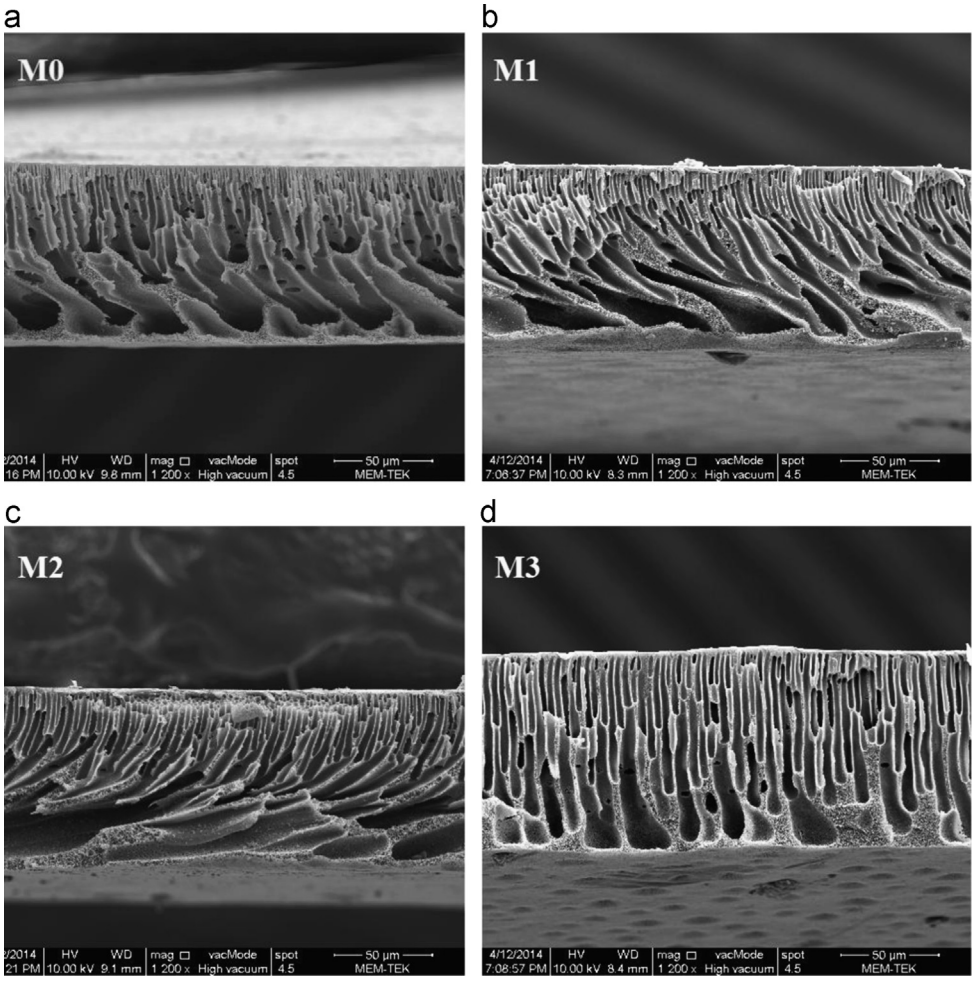

Fig. 3. Cross-sectional SEM images of the blend membranes (a) M0; (b) M1; (c) M2 and (d) M3.

The hydraulic resistance of the membrane (R_m) was evaluated from the slope of the transmembrane pressure difference (ΔP) vs. pure water flux (J_w) plot using the following equation:

$$J_w = \frac{\Delta P}{R_m} \tag{4}$$

2.3.3. Membrane solute rejection and antifouling performance

The solute rejection performance of prepared membranes were studied by using BSA as a model protein. BSA was dissolved in phosphate buffer (0.05 M, pH 7.0) solution and its concentration was adjusted as 500 mg L^{-1} for all experiments. The rejection of BSA was carried out at 200 kPa for all blend membranes. The BSA rejection ratio was calculated by the following equation:

$$R\,(\%) = \left(1 - \frac{C_p}{C_f}\right) \times 100 \tag{5}$$

where, C_p and C_f are the concentrations in permeate and the feed respectively.

After BSA rejection experiments, the membranes were washed with deionized water and immersed in distilled water for 20 min for cleaning. Then the pure water flux of cleaned membranes was measured. The flux recovery ratio (FRR) was calculated using Eq. (6).

$$FFR\,(\%) = \left(\frac{J_{w1}}{J_{w2}}\right) \times 100 \tag{6}$$

where, J_{w1} is the PWF of pristine membrane and J_{w2} is the PWF cleaned membranes after BSA rejection experiments.

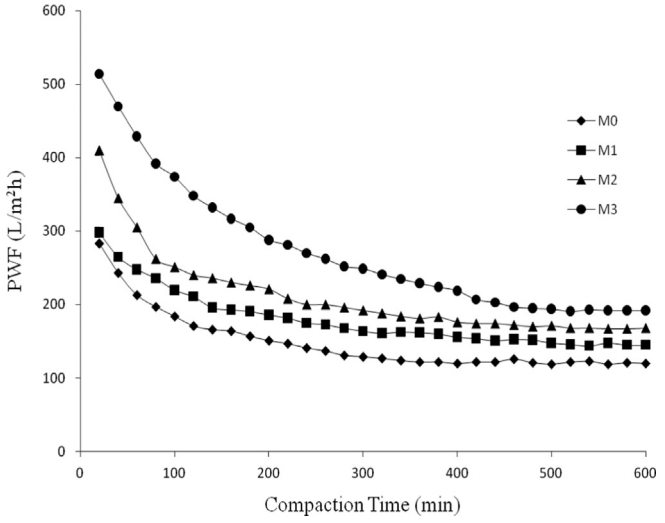

Fig. 4. The effect of compaction time on PWF values for PSf and PSf/PBI blend membranes.

2.3.4. Antibacterial studies

Antibacterial ability of the blend membranes were determined by a modified Kirby-Bauer disc diffusion method [16] under standard conditions using Mueller-Hinton agar medium, regarding to the recommendations of the National Committee of Clinical Laboratory Standards, NCCLS. The anti-biofouling ability was carried out using culture of *Bacillus cereus* ATCC7064, *Staphylococcus aureus*

Table 3
Some characterization parameter values of PSf and PSf/PBI blend membranes.

Membrane	% Water content	% porositiy	Contact angle (°)	PWF at 200 kPa (L/m^2 h)	BSA rejection (%)	Flux recovery ratio (FRR) (%)	Compaction factor (CF)	Hydroulic resistance (R_m) (m^2 h kPa/L)
M0	74.53 ± 0.81	62.50 ± 1.94	60.04 ± 0.40	228 ± 18	35.74 ± 2.06	78.2 ± 2.8	2.33	0.61
M1	76.96 ± 0.66	68.55 ± 1.91	57.33 ± 1.50	254 ± 15	56.88 ± 1.35	92,7 ± 3.5	2.06	0.48
M2	77.34 ± 2.09	70.25 ± 1.89	54.15 ± 1.40	280 ± 18	62.40 ± 2.55	92,9 ± 3.5	2.44	0.44
M3	82.70 ± 0.80	75.28 ± 2.14	51.54 ± 1.40	355 ± 16	68.66 ± 2.34	93,5 ± 5.2	2.68	0.39

ATCC 25923 as Gram positive bacteria and *Escherichia coli* ATCC 25922, *Pseudomonas aeruginosa* ATCC 27853 as Gram negative bacteria. These clinical type strains were collected from NRLL-B and ATCC culture collections.

Petri dishes (measuring 90 mm each side) containing 20 ml Mueller Hinton agar (Oxoid) were prepared. Each test isolate was checked for its purity in nutrient agar (NA-Merck), and several colonies were emulsified into 5 ml Nutrient Broth (NB-Merck), and adjusted spectrophotometrically to 0.1 absorbance at OD_{600}. The final concentration of inoculum was regulated to 10^5 CFU/mL (0.5 McFarland standard, Vitek colorimeter). 200 μl of bacterial suspension was pipetted into an agar plate and then spreaded on Mueller Hinton agar surface by using sterile swab under the sterile conditions.

The membranes blended with PBI and bare were cut aseptically into 6 mm diameter discs and then were irradiated with ultra violet radiation for 30 min to ensure that they were sterile. The membranes were placed gently on the agar surface to cover an area in the middle of the plate. The plates were incubated at 37 °C for 24 h. The diameter of inhibition zone was measured in millimeters by compass. All assays were replicated three times to minimize test error.

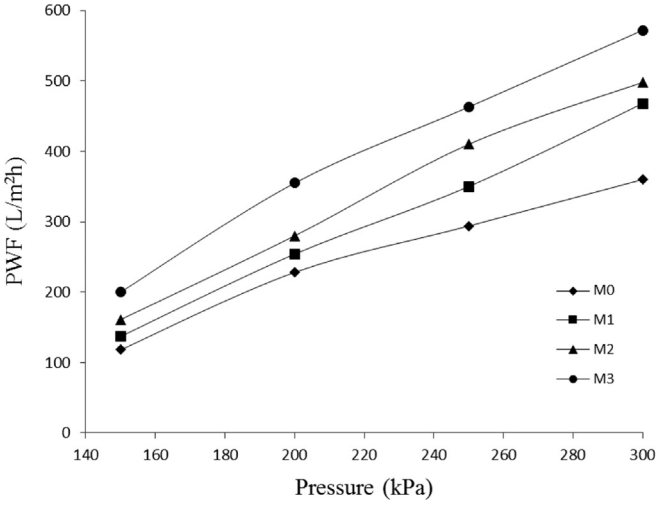

Fig. 5. The effect of transmembrane pressure on PWF values for PSf and PSf/PBI blend membranes.

3. Result and discussion

3.1. FTIR analysis of membranes

FTIR spectra of the membranes were shown in Figs. S1 and S2 (see the figures in the supplementary file). M0 membrane exhibited the bands at 1294 and 1149 cm^{-1}, signifying the symmetric stretching vibration of O═S═O group. The bands at 2874, 2970 and 3096 cm^{-1} indicated the presence of CH_3-symmetric aliphatic stretching, CH_3-asymmetric aliphatic stretching and C–H aromatic stretching, respectively [17–18]. The band at 1585 cm^{-1} is characteristic of C═C conjugation of the aromatic ring. After blending process with PBI, the bands at 3365 and 1642 cm^{-1} exhibiting strong adsorption of water became more pronounced. Further, the O═S═O group stretching frequencies at 1294 and 1149 cm^{-1} of PSf shifted to 1293 and 1150 cm^{-1} respectively. This shift confirmed the establishment of hydrogen bond between the N^+–H of PBI and S═O of PSf. The occurrence of such interactions was initiated by the transfer of lone pair of electron present in the oxygen of sulfone group. The possible interactions and the established hydrogen bonds between PSf and PBI were represented in Scheme 2. The formation of this intermolecular hydrogen bonding favored the good miscibility between PSf and PBI and homogeneity at molecular scale in blend membranes.

3.2. Thermal analysis of membranes

The TG/DTG and DSC techniques were used to evaluate the thermal stability and miscibility of the blend membranes. The TG curves of PSf membranes in air were shown in Fig. 1. To compare the results of the decomposition characteristics in a more quantitative way, the nonisothermal decomposition data of membranes at various heating rates in air were summarized in Table 2. The

Table 4
Measured inhibition zone in diameter (mm) of PBI membrane and bare membrane on some Gram positive bacteria and Gram negative bacteria by disk diffusion method.

Compound	*E. coli*	*S. aureus*	*P. aeroginosa*	*B. subtilis*
Inhibition zone radius (mm)				
M0	–	–	–	–
M3	8	10	14	–

thermal degradation of PSf and PSf/PBI blends occurred in three steps between 80 and 650 °C. The first mass loss was observed about 90 °C attributed to the removal of water and solvent traces. The second and third mass losses occurring at temperature above 400 °C may be due to the degradation of polymer main chain [19,20]. As given in Table 2, T_{onset}, T_{max} and $(d\alpha/dt)_{max}$ values for all membranes increased progressively with increasing heating rate. The increase of the onset decomposition temperature does not mean that the thermal stability of the membranes has increased. It is mainly due to a kinetics effect, i.e. the thermal response of the membranes is delayed at fast heating rates. The shift of the TG curves to the higher temperature with increasing heating rate could be attributed to the short time required for a sample to reach a given temperature at high heating rate. At the same heating rate, it is interesting to note that T_{max1} and T_{max2} of blend membranes are generally lower than that of M0. The maximum mass-loss rates $(d\alpha/dt)_{max1}$, for the first weight-loss step of M0 is much higher than that of the blend membranes. These differences could be explained by an enhanced asymmetry in the polysulfone structure.

The DSC curves for the PSf and PSf/PBI blend membranes were shown in Fig. 2. At the heating rate of 10 °C/min, the T_g of the M0 was determined as 147 °C. This result was lower than the results obtained from previous studies [21–23]. This inconsistency may be due to the experimental conditions that the samples were prepared,

Table 5
Comparison of PBI blended PSf membrane with literature.

Membrane type	PWF (L/m^2 h)	BSA rejection (%)	FFR (%)	Ref.
% 20 N-succinyl chitosan blended PSf	228.2 (at 200 kPa)	93.5	70.0	[3]
% 0.1 Polyaniline blended PSf	230 (at 200 kPa)	98.0	78.5	[29]
% 5 N-propylphosphonic Chitosan blended PSf	230 (at 200 kPa)	94.0	74.0	[30]
% 1 $CaCO_3$ blended PSf	60 (at 200 kPa)	90.0	51.0	[31]
% 0.01 Emeraldine base polyaniline blended PSf	175 (at 200 kPa)	98.0	65.0	[32]
% 0.5 TiO_2 blended PSf	61 (at 200 kPa)	93.0	68.0	[33]
% 0.5 N-vinylcaprolactam-co-acrylic acid blended PSf	1.41 (at 150 kPa)	90.0	64.9	[34]
% 1 PBI blended PSf	355 (at 200 kPa)	68.7	93.5	In this study

such as the coagulation bath and its temperature. The DSC analysis showed that the T_g values of PSf/PBI blends gradually increased and shifted to higher temperatures with increasing the mass ratio of PBI. These changes in T_g were due to the specific interactions between the two polymer components as shown in Section 3.1. The single T_g for each sample suggested that the blends have good miscibility over the whole range of studied composition ratio.

3.3. SEM analysis of membranes

Fig. 3 presented the cross-section SEM images of membranes with different PBI mass ratios. This images showed that PSf and all the PSf/PBI blend membranes had finger-like structure having good interconnection. Observed changes on the morphology of blend membranes were attributed to the reduced interactions between PSf chains. This was due to the addition of PBI to the casting solution leads to formation of hydrogen bonds between hydrogen atom of N^+–H group on PBI and oxygen atom of sulfone group on PSf; therefore, the interactions between PSf chains were reduced. Moreover, due to the hydrophilicity of PBI and formation of hydrogen bonding between PBI and NMP (solvent), the rate of the solvent outflow decreased and the non-solvent (water) inflow increased [24,25]. Both phenomena resulted in a delay in the concentration rate of the polymer on the surface. Consequently, the growth of skinlayer diminished and formation of finger-like pores in the membrane improved.

3.4. Flux, rejection and antifouling analysis

For all the membranes, it was observed that the PWF decreased gradually with time due to compaction and finally attained a steady state after 6–7 h (Fig. 4). Compared with the initial water flux, the steady water fluxes decreased at the rate of 57.6%, 51.3%, 59.0%, and 67.9% for M0, M1, M2 and M3, respectively. This was due to the fact that the walls of the pores became closer, denser and uniform during compaction. The pure water flux of the M3 membrane is the best among 4 types of the membranes under different compaction time and pressures. This is due to the enhancing porosity and hydrophilicity with increasing the PBI additive.

Contact angle and water uptake studies were carried out to show the hydrophilicity, roughness and porosity of the surface. It can be seen from Table 3 that contact angle decreased with increase in the PBI amount. The contact angle results were relatively smaller than the ones that were expected for PSf membranes [26–29]. This was probably related to the higher porosity, roughness and the hydrophilicity of the surface. As given in Table 3, the highest water uptake observed was 82.7% and the minimum of 74.5%. Membrane with highest percentage of PBI showed maximum water uptake. This provided an evidence for the fact that the increase of PBI amount in the membrane component increased the hydrophilic nature of the membrane. The presence of 0.5 mass% of PBI in the membrane, the water flux enhanced from 254 to 280 and reached to 355 L m^{-2} h^{-1} at 1.0 mass% of PBI (Fig. 5). BSA rejection capabilities were determined to investigate the performance of membranes. The BSA rejection values for M0, M1, M2 and M3 were calculated as 37.7%, 56.9%, 62.4% and 68.7 %, respectively (Table 3). This results showed that the blend membranes have higher pure water flux and BSA rejection than PSf membrane. This can be explained by the decreasing pore size while increasing porosity and hydrophilicity. The flux recovery ratio (FRR) values for membranes after UF of BSA solution are presented in Table 3. The FRR value for membrane M0 after UF of BSA solution was found to be 78.2 ± 2.8 %, which is the lowest among all membranes. The FRR values were improved with modification with PBI. This could be attributed to the membrane fouling arised from hydrophobic interactions between BSA and membrane. It means that the modification of PSf membrane with PBI additive improved the fouling resistance. This results showed the contribution of concentration polarization is not important to the observed rejection, this increasing can be attributed to membrane pore size properties.

3.5. Antibacterial tests

The antibacterial ability of the M0 and M3 membrane were tested, and the results are presented in Table 4. The results indicated that PBI indeed acted as a strong bacterial-killing against *E. coli*, *S. aureus* and *P. aeroginosa*, showed a weak bacterial-killing capacity against *B. subtilis*. This study showed that the PSf/PBI membrane has the potential to reduce bio-fouling in water treatment.

3.6. Comparison of the prepared membranes with literature

Table 5 compares PWF, BSA rejection and FFR values of the present membranes with those of the literature data [3,29–34]. A comparison of all the membranes was made under similar feed conditions. On comparison, we find that the present membranes offered the highest FFR value.

4. Conclusion

With the addition of PBI, the membrane morphology was altered and also the hydrophilicity and porosity of membrane were increased. The improving hydrophilicity of the PSf/PBI membranes were proved by decreasing contact angle and increasing permeation results. The change in the hydrophilicity of PSf after addition of PBI was attributed to the hydrophilic NH groups of PBI. Porosity values of M0 and M3 membranes were 62.5% and 75.28% respectively. PWF of M1, M2 and M3 were 1.17, 1.23 and 1.56 times higher, and rejection of M1, M2 and M3 were 1.59, 1.75, 1.92 times higher that of M0, respectively. This is because of PSf/PBI blend membranes have more hydrophilic surface and higher porosity but smaller pore size than PSf membrane. PBI blended PSf membranes showed a distinct two-step degradation process between 400 and 600 °C.

These two steps are similar to the steps obtained from PSf membranes. The changes in T_g proved the presence of interaction between Psf and PBI components. The decreased contact angle of blended membranes indicated that the addition of PBI enhanced membrane surface hydrophilicity, which might be attributed to the hydrophilic group of PBI (N^+–H). This is mainly due to the entrapment of PBI in the membrane which leads to the decrease of contact angle. The anti-biolfouling ability against Gram positive bacteria and Gram negative bacteria was studied for M0 and M3 membranes. The observed results can be attributed to the hydrogen bonds with the active centers of the cell constituents through the N–H group on benzimidazole ring.

Acknowledgments

We thank Dr. Murat Erdem for the instrumentation about the SEM images, and Dr. Bülent ÇAĞLAR for the instrumentation about the DSC measurements. We would like to thank Prof. Dr. Andrew Zydney (The Pennsylvania State University, USA) and Reviewers for their remarks and corrections of the manuscript.

Appendix A. Supporting information

Supplementary data associated with this article can be found in the online version at http://dx.doi.org/10.1016/j.memsci.2014.10.010.

Nomenclature

A	effective membrane surface area (m^2)
BSA	bovine serum albümin
Cf	concentrations in feed
CF	compaction factor
C_p	concentrations in permeate
d	density of water in wet membrane
$(d\alpha/dt)_{max}$	maximum mass-loss rate
Da	dalton
$DAB \cdot 4HCl \cdot 2H_2O$	3,3′-diaminobenzidine tetrahydrochloride
DSC	differential scanning calorimetry
DTG	derivative thermogravimetry
FRR	flux recovery ratio
FTIR–ATR	Fourier transform infrared spectroscopy-attenuated total reflectance
IPA	isophthalic acid
J_{w1}	pure water flux, L/m^2 h
J_{w2}	pure water flux after rejection, L/m^2 h
m^2	square meter
Mw	molecular weight
NCCLS	National Committee of Clinical Laboratory Standards
NMP	*N*-methyl-2-pyrrolidone
Pa	Pascal
PBI	poly[2,2′-(m-phenylene)-5,5′-dibenzimidazole]
PEG-400	polyethylene glycol 400
PPA	polyphosphoric acid
PSf	polysulfone
PWF	pure water flux, L/m^2 h
R	rejection (%)
R_m	hydraulic resistance of the membrane
SEM	scanning electron microscope
TG	thermogravimetry
T_g	glass transition temperature
T_{max}	temperature at the maximum mass-loss rate
T_{onset}	onset temperature
UF	ultrafiltration
V	volume of the wet membrane
W_d	dry membrane's weight
W_w	wet membrane's weight
ΔP	transmembrane pressure difference
Δt	sampling time (h)

References

[1] A. Cassano, C. Conidi, E. Driol, Physico-chemical parameters of cactus pear (Opuntia ficus-indica) juice clarified by microfiltration and ultrafiltration processes, Desalination 250 (2010) 1101–1104.
[2] A.M. Urtiaga, G. Pérez, R. Ibáñez, I. Ortiz, Removal of pharmaceuticals from a WWTP secondary effluent by ultrafiltration/reverse osmosis followed by electrochemical oxidation of the RO concentrate, Desalination 331 (2013) 26–34.
[3] R. Kumar, A.M. Isloor, A.F. Ismail, T. Matsuura, Performance improvement of polysulfone ultrafiltration membrane using N-succinyl chitosan as additive, Desalination 318 (2013) 1–8.
[4] W. Zhang, G. Huang, J. Wei, D. Yan, Gemini micellar enhanced ultrafiltration (GMEUF) process for the treatment of phenol wastewater, Desalination 311 (2013) 31–36.
[5] M. Padaki, A.M. Isloor, A.F. Ismail, M.S. Abdullah, Synthesis, characterization and desalination study of novel PSAB and mPSAB blend membranes with Polysulfone (PSf), Desalination 295 (2012) 35–42.
[6] M. Padaki, A.M. Isloor, P. Wanichapichart, A.F. Ismail, Preparation and characterization of sulfonated polysulfone and N-phthloyl chitosan blend composite cation-exchange membrane for desalination, Desalination 298 (2012) 42–48.
[7] M.Z. Yunos, Z. Harun, H. Basri, A.F. Ismail, Studies on fouling by natural organic matter (NOM) on polysulfone membranes: effect of polyethylene glycol (PEG), Desalination 333 (2014) 36–44.
[8] R. Kumar, A.M. Isloor, A.F. Ismail, T. Matsuura, Performance improvement of polysulfone ultrafiltration membrane using N-succinyl chitosan as additive, Desalination 318 (2013) 1–8.
[9] G. Kalaiselvi, P. Maheswari, S. Balasubramanian, D. Mohan, Synthesis, characterization of polyelectrolyte and performance evaluation of polyelectrolyte incorporated polysulfone ultrafiltration membrane for metal ion removal, Desalination 325 (2013) 65–75.
[10] R. Kumar, A.M. Isloor, A.F. Ismail, S.A. Rashid, A. Ahmed, Permeation, antifouling and desalination performance of TiO_2 nanotube incorporated PSf/CS blend membranes, Desalination 316 (2013) 76–84.
[11] M. Homayoonfal, A. Akbari, M.R. Mehrnia, Preparation of polysulfone nanofiltration membranes by UV-assisted grafting polymerization for water softening, Desalination 263 (2010) 217–225.
[12] Z. Zhang, Z. Wang, J. Wang, S. Wang, Enhancing chlorine resistances and antibiofouling properties of commercial aromatic polyamide reverse osmosis membranes by grafting 3-allyl-5,5-dimethylhydantoin and N,N′-Methylene-bis(acrylamide), Desalination 309 (2013) 187–196.
[13] D.Y. Xing, S.Y. Chan, T.S. Chung, Fabrication of porous and interconnected PBI/P84 ultrafiltration membranes using [EMIM]OAc as the green solvent, Chem. Eng. Sci. 87 (2013) 194–203.
[14] T.S. Chung, W.F. Guo, Y. Liu, Enhanced Matrimid membranes for pervaporation by homogenous blends with polybenzimidazole (PBI), J. Membr. Sci. 271 (2006) 221–231.
[15] Y. Wang, M. Gruender, T.S. Chung, Pervaporation dehydration of ethylene glycol through polybenzimidazole (PBI)-based membranes, J. Membr. Sci. 363 (2010) 149–159.
[16] A.W. Bauer, M.M. Kirby, J.C. Sherris, M. Truck, Antibiotic susceptibility testing by a standardized single disk method, Am. J. Clin. Pathol. 45 (1996) 493–496.
[17] B.M. Ganesh, A.M. Isloor, A.F. Ismail, Enhanced hydrophilicity and salt rejection study of graphene oxide-polysulfone mixed matrix membrane, Desalination 313 (2013) 199–207.
[18] M. Padaki, A.M. Isloor, P. Wanichapichart, Polysulfone/N-phthaloylchitosan novel composite membranes for salt rejection application, Desalination 279 (2011) 409–414.
[19] F. Lufrano, I. Gatto, P. Staiti, V. Antonucci, E. Passalacqua, Sulfonated polysulfone ionomer membranes for fuel cells, Solid State Ion. 145 (2001) 47–51.
[20] X.G. Li, M.R. Huang, Thermal degradation of bisphenol A polysulfone by high-resolution thermogravimetry, React. Funct. Polym. 42 (1999) 59–64.
[21] Z. Yi, L.P. Zhu, Y.F. Zhao, B.K. Zhu, Y.Y. Xu, An extending of candidate for the hydrophilic modification of polysulfone membranes from the compatibility consideration: the polyethersulfone-based amphiphilic copolymer as an example, J. Membr. Sci. 390–391 (2012) 48–57.
[22] C. Camacho-Zuñiga, F.A. Ruiz-Treviño, S. Hernández-López, M.G. Zolotukhin, F.H.J. Maurer, A. González-Montiel, Aromatic polysulfone copolymers for gas separation membrane applications, J. Membr. Sci. 340 (2009) 221–226.

[23] M. Peyravi, A. Rahimpour, M. Jahanshahi, Thin film composite membranes with modified polysulfone supports for organic solvent nanofiltration, J, Membr. Sci. 423–424 (2012) 225–237.
[24] R. Naim, A.F. Ismail, A. Mansourizadeh, Effect of non-solvent additives on the structure and performance of PVDF hollow fiber membrane contactor for CO_2 stripping, J. Membr. Sci. 423–424 (2012) 503–513.
[25] Q. Wang, Z. Wang, Z. Wu, Effects of solvent compositions on physicochemical properties and anti-fouling ability of PVDF microfiltration membranes for wastewater treatment, Desalination 297 (2012) 79–86.
[26] M. Wang, L.G. Wu, J.X. Mob, C.J. Gaoa, The preparation and characterization of novel charged polyacrylonitrile/PES-C blend membranes used for ultrafiltration, J. Membr. Sci. 274 (2006) 200–208.
[27] M. Temtema, T. Casimiro, J.F. Manob, A. Aguiar-Ricardo, Preparation of membranes with polysulfone/polycaprolactone blends using a high pressure cell specially designed for a CO2-assisted phase inversion, J. Supercrit. Fluid 43 (2008) 542–548.
[28] X. Wei, Z. Wang, J. Wang, S. Wang, A novel method of surface modification to polysulfone ultrafiltration membrane by preadsorption of citric acid or sodium bisulfite, Membr. Water Treat. 3 (2012) 35–49.
[29] Z. Fan, Z. Wang, N. Sun, J. Wang, S. Wang, Performance improvement of polysulfone ultrafiltration membrane by blending with polyaniline nanofibers, J. Membr. Sci. 320 (2008) 363–371.
[30] R. Kumar, A.M. Isloor, A.F. Ismail, T. Matsuura, Synthesis and characterization of novel water soluble derivative of Chitosan as an additive for polysulfone ultrafiltration membrane, J. Membr. Sci. 440 (2013) 140–147.
[31] A.K. Nair, A.M. Isloor, R. Kumar, A.F. Ismail, Antifouling and performance enhancement of polysulfone ultrafiltration membranes using $CaCO_3$ nanoparticles, Desalination 322 (2013) 69–75.
[32] S. Zhao, Z. Wang, X. Wei, B. Zhao, J. Wang, S. Yang, S. Wang, Performance improvement of polysulfone ultrafiltration membrane using PANiEB as both pore forming agent and hydrophilic modifier, J. Membr. Sci. 385–386 (2011) 251–262.
[33] G. Zhang, S. Lu, L. Zhang, Q. Meng, C. Shen, J. Zhang, Novel polysulfone hybrid ultrafiltration membrane prepared with TiO_2-g-HEMA and its antifouling characteristics, J. Membr. Sci. 436 (2013) 163–173.
[34] M.K. Sinha, M.K. Purkait, Preparation and characterization of stimuli-responsive hydrophilic polysulfone membrane modified with poly (N-vinyl-caprolactam-co-acrylic acid), Desalination 348 (2014) 16–23.